EUROPEAN ACADEMIC RESEARCH
Vol. VII, Issue 3/ June 2019

Impact Factor: 3.4546 (UIF)
DRJI Value: 5.9 (B+)

ISSN 2286-4822
www.euacademic.org

Correlation between Corrosion and Ferrite Number of 316L Stainless Steels Deposited on Carbon Steel Aged at 550° C

AMANY NAGY KAMEL
Quality Control and Quality Assurance Department
Egyptian nuclear and radiological regulator authority (ENRRA)
A. F. WAHEED
Metallurgy Department, Nuclear Research Center
Atomic Energy Authority, Cairo, Egypt

Abstract

The good oxidation and corrosion resistance of stainless steels (SS), they are excellent candidates for their usage in nuclear reactors as pressurized water reactors. The delta ferrite content in the weld metal plays an important role in determining the fabrication and service performance of the welded structures. The ferrite morphology will depend on the weld section viewed. Studies have been carried out to evaluate the microstructure of (316L SS) metal deposited on carbon steel in the as weld condition and aging times 50,500 and 1000 hr at 550°C. The weld metal close to this fusion boundary had a cellular structure, by using Schaeffler diagram it can be predicting the first-pass weld microstructure for used (316L SS) and the ferrite numbers (FN). The corrosion behavior of 316L in an aggressive media namely NaCl 3% at room temperature was tested. The stainless steels were examined through potentiodynamic polarization curves. The results indicate that the major corrosion type that has been observed for all samples was localized corrosion. The corrosion current density (I_{corr}) of different conditions of the samples varied in a very wide range, from is 5.2 E-3(A/ cm²) to 6.44E-6 (A/ cm²) and the highest corrosion current density (I_{corr}) is for as weld condition. There were differences in the

corrosion potential (E_{corr}) values for the samples aged at 550 ˚C and the as weld condition.

Keywords: Stainless steel AISI (316 LSS), carbon, steel, corrosion, aging and ferrit numbers

1. INTRODUCTION

Stainless steels are used extensively in the nuclear, battery, automotive and defense industries, because of their excellent strength, oxidation characteristics and acceptable corrosion resistance. [1-2-3]. These properties are primarily due to the presence of chromium and Nickel as alloying elements. Chromium is classified as a strategic material because it imparts corrosion resistance. Stainless steel filler metal that has a 30% higher coefficient of thermal expansion than ordinary steel can be used in welding [4]. There has been a considerable amount of interest in a search for stainless steels; it is well known that Ni extends the γ-loop in iron-carbon equilibrium diagram. On the other hand, Cr is a α-stabilizer element, Cr is a carbide forming element, therefore, the level of carbon is very sensitive due to the strong affinity of Cr to form carbide which impair the corrosion behavior [5-6].

Type (316LSS) substitutes approximately 2% Mo for a nearly equal amount of Cr to improve pitting corrosion behavior [7]. The L grades represent low-carbon variants with a nominal carbon level of 0.03 % depending on the specification to which it is manufactured, which are used for general stainless steel fabrications, elevated temperature applications and resistance to pitting corrosion respectively [8]. 300 series of austenitic stainless steels usually solidify during welding as a mixture of austenite and ferrite. The ferrite almost fully transforms to austenite on cooling, but there could be retention of a few percent of δ ferrite in the weld metal [9]. More than 2% δ ferrite phase is presented in type 316L stainless steels due to improvement of hot workability or welding process [10-11]. In this paper, the effect of the aggressive media, namely, 3% NaCl on the corrosion behavior of this layer of (316LSS) deposited on carbon steel will be tested, by conducting corrosion tests, microscopic structure and ferrite number of these layers.

2. MATERIALS AND SPECIMENS PREPARATION

2.1 Material of plates and Filler metal

The coated electrode of class AWS (American Welding Society) was used in the welding experiments. The type are (E-316LSS) with diameter ϕ =4 mm. The chemical composition of the plates and electrode used are shown in Table (1).

Table (1) the chemical composition of the plates and electrodes

Element	C	Si	Mn	Cr	Ni	Mo	P	S	Fe
Carbon steel (CS)	0.2	0.23	1.37	0.01	0.01	0.005	0.02	0.008	Basis
E 316 L	<0.003	0.8	0.8	18.5	12	2.6	-	-	Basis

2.2 Weld metal deposit

Welding process with SMAW, electrode diameter 4 mm, AWS E (316LSS) with one pass. The welding current is120~140A. Polarity DCEP and welding voltage is 60 V.

2.3 Metallographic examination

The weld deposit (316LSS) and carbon steel were metallographic examinaed. The specimens were prepared by grinding under water on rotating disc, using abrasive paper with grades ranging from 180 to 2000. Then polished to mirrored surface by using diamond paste with grades 3 and 1 micron.

The microstruructure for as weld conditions and after aging were examined. The deposited stainless steel (316LSS) was electrolytically etched with the condition (10g oxalic acid, 6Vdc, 15-30 s) and Carbon steel was etched with 2% Nital. Specimens were rinsed with alcohol and dried with hot air. The optical microscope (OM) was used for microstructural examination.

2.4 Electrochemical Corrosion testing

The specimens were ground on SiC grinding papers from 240 till 1000 grade, followed by polishing on polishing lapped cloth using 1µm diamond suspension. Then the polished specimens were degreasing with ethanol before immersion in the test solution. The electrochemical corrosion behavior of the specimens were studied by applying the Potentiodynamic polarization technique using a potentiostat (Electrochemical Impedance Analyzer, Model 6310)

interfaced to a computer and a three-electrode cell with the working electrode of exposed area 100 mm2, a saturated calomel reference electrode (SCE), carbon electrode as counter electrode. The testing media was 3% NaCl prepared from duple distilled water and reagent grade salt. The surface area of (316LSS) is equal to (carbon steel) CS area which is immersed in the test solution; the rest of CS was covered with plastic tap.

2.5 Ferrite Number Equipment:

For determination the ferrite number of weld metal at the as weld condition by using the three diagrams Schaeffler diagram [12],DeLong diagram[13] and the WRC-1992 diagram[14]

3. RESULTS AND DISCUSSION

3.1 Microstructure

Concerns about dissimilar metal welding, weld metal constitution center around the first weld pass or root pass, primarily because of dilution effects are greatest in this pass. In many cases of dissimilar metal welding, a highly desirable goal in selecting the filler metal is, to obtain stable austenite with a small amount of ferrite in this first weld pass. In the case of 316L stainless steel,the C, Mn, Ni, and N concentrations were responsible for the low ferrite number proving to be strong austenite stabilizers. The elements Cr, Si and Mo, on the other hand, are known as strong ferrite stabilizers and increase the ferrite number[15]. The microstructure of stainless steels (316LSS) weld metal deposited on carbon steel in the as weld condition and aged specimens at times 50,500 and 1000 hr at 550°C are shown in Figure (1).

The as welded condition showed that the microstructure consists of austenite (white phase) as a matrix and the ferrite as the second phase (which appears as black phase) for weld metal type (316LSS). In the stainless steel side and at the fusion boundary[16], crystal orientation of the base metal has great influences on the microstructure of the weld and cause to form the epitaxial growth region. The epitaxial growth zone is very narrow and its size is restricted due to the high thermal gradient produced between the base metal and the fusion zone.

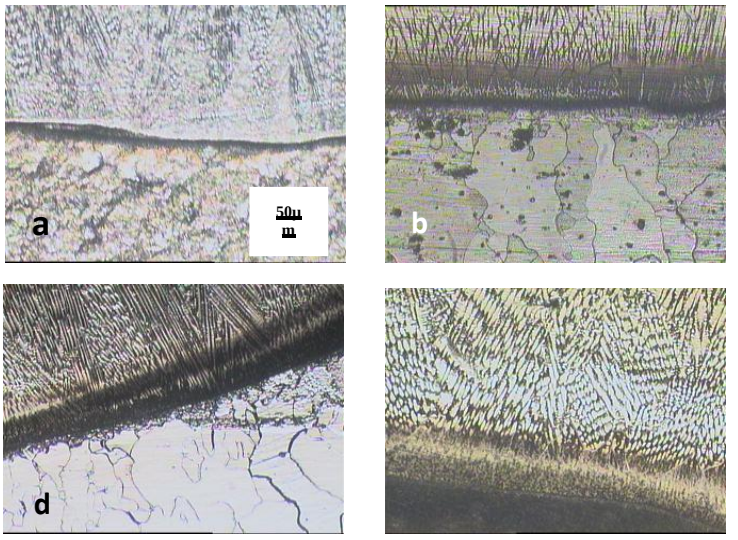

Figure (1) 316L Optical micrograph showing the microstructure features of 316L weld metal deposited on carbon steel (a) as weld (b) 50 hr aging (c) 500 hr aging and (d) 1000 hr aging.

For welding purposes, it is therefore important to take into consideration that the weld metal ferrite content was vermicular and lathy. At 550◦C delta ferrite will undergo transformation and segregate into ferromagnetic delta ferrite and paramagnetic delta ferrite. [17- 18].

Close to the fusion boundary, the SS clad region consisted of a narrow zone of fine dendrites of ferrite and austenite as shown in Figure (1). The weld metal close to this fusion boundary had a cellular structure, which was different from that observed in the CS side. This suggests that there could be compositional differences in these two regions, and the mode of solidification could have also been different. However, the microstructural features of the weld metal, observed near the fusion boundary of SS and CS sides, even though close to the fusion boundary were distinctly different [19-1].

3.2 Ferrite number

The ferrite(δ-ferrite) phase content in stainless steel weldments expressed in terms of Ferrite Number (FN) has proven very valuable in assessing the performance and predicting microstructure of austenitic stainless steel. 2- 4% delta-ferrite(δ-ferrite) phase is

presented in fully austenitic stainless steels (SS) such as type 316L SS because δ-ferrite phase is intentionally formed during manufacturing to improve welding[20]. More than 4% δ-ferrite phase is formed during non-equilibrium solidification. The effects of δ-ferrite phase on the corrosion resistance of austenitic SS were explained with the following; the formation of Cr-depleted zone [21], low concentrations of Cr and Mo in γ□phase [22]. The 300 series of austenitic stainless steel is primarily monophasic at room temperature. (FN) is controlled by several factors and is the result of the series of microstructural changes that take place during the welding process [23] Thus, the relationship between the alloy composition and the ferrite content can be quite complex. The relative influence of each alloying addition given by element coefficients in the Cr_{eq} or Ni_{eq} expression is likely to change when there is a change in the base composition. In this study the Cr_{eq} = 22.3% and Ni_{eq}= 12.49% and the aging temperature was550 C, at different times. At these conditions the ferrite in the microstructure is a small fraction included in austenite matrix.[24]

The Schaeffler diagram is an important tool for predicting the constitution of austenitic Cr-Ni steel welds with carbon contents up to 0.12 %. However, it does not allow determination of the composition and volume of the carbide phase. Furthermore, if the carbon content in a weld exceeds 0.12 %, the agreement of predictions with actual data is markedly reduced due to an intense consumption of carbon and carbide-forming elements by the carbide formation process.

The diagram is based on the fact that the alloying elements can be divided into ferrite stabilisers and austenite-stabilisers. This means that they favour the formation of either ferrite or austenite in the structure. If the austenite-stabilisers ability to promote the formation of austenite is related to that for nickel, and the ferrite-stabilisers likewise compared to chromium, it becomes possible to calculate the total ferrite and austenite stabilising effect of the alloying elements in the steel. This gives the so-called chromium and nickel equivalents.

The Schaeffler diagram [12] Figure (2), DeLong diagram [13] Figure (3-a) and the WRC-1992 diagram [14] Figure (3-b) can be used to predict weld metal and transition region microstructure during dissimilar metal welding of stainless steels. Table (2) show the FN of weldment (316LSS) by using the three diagrams.

Table(2)show the FN of weldment 316L by using the three diagrams

Constitution Diagram	**Cr_{eq} and Ni_{eq}**	**Cr, Ni Equivalent 316L**	**FN 316L**
Shaeffler diagram[ ] Figure (3)	Cr_{eq} =Cr+Mo+1.5 Si Ni_{eq} = Ni+30C+0.5Mn	Cr eq. =22.3 Ni eq=12.49	10
DeLong diagram[ ] Figure (3)	Cr_{eq} =Cr+Mo+1.5 Si Ni_{eq} = Ni+30C+30N+0.5Mn	Cr eq=22.3 Ni eq=12.49	17
WRC 1992 [ ] Figure (3)	Cr_{eq} =Cr+Mo Ni_{eq} =Ni+35C+20N+ 0.25 Cu	Cr eq=21.4 Ni eq=12.105	16

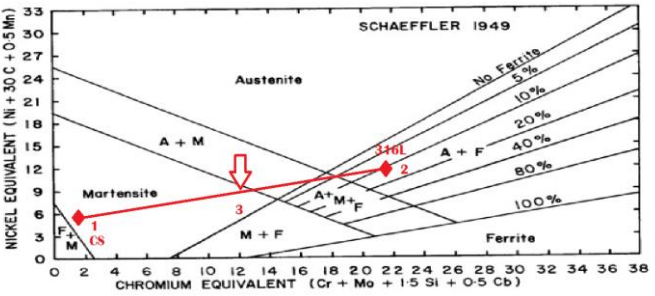

.Figure (2) Schaeffler diagram

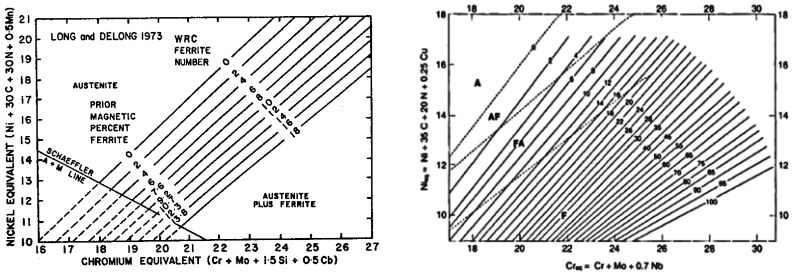

Figure (3)DeLong diagram (a) and the WRC-1992 diagram (b)

By using Schaeffler diagram it can be followed in predicting the first-pass weld microstructure for use (316L SS) filler metals. The tie-line from the (316LSS) point 1 composition in Figure (2-a) to the synthetic base metal composition point 2 is within the area of the diagram indicating that ferrite will be present 10%. With Type (316LSS) filler metal, the weld deposit will be almost certainly fully austenitic, unless dilution 50% point 3 by the base metals is extremely high, in which case martensite not ferrite will appear. Tie-line can also be

used to predict the microstructure in the transition region at the fusion boundary. All these microstructures can be expected in a narrow region between the base metal HAZ and the fully mixed weld metal.

3.3 Potentiodynamic Polarization Tests

The corrosion current density I_{corr} and corrosion potential E_{corr} of (316LSS), which was determined by potentiodynamic technique are shown in Table (3). From these data, it can be generally evaluate the corrosion performance of (316LSS) at different aging conditions.

Table (3) Corrosion potential E_{corr} and corrosion current density I_{corr} for 316L

Aging condition	E_{corr} (mV)	Icorr (A/cm2)
As weld	-514	1.35E-3
***50*hr**	-583.7	5.2E-3
500hr	-462.1	6.44E-6
1000hr	-785.3	560.2E-6

The electrochemical tests were established by using Potentiodynamic technique at room temperature. Anodic polarization curves for specimens (316L SS and CS) for as weld condition and aging times 50,500 and 1000 hr at 550 ^{0}C in 3% NaCl solution having neutral pH are shown in Figures (4-7).

In Figure (4) for as weld specimen the corrosion current density I_{corr} is 1.35 E-3(A/ $cm^{2)}$, the current density increases moderately till -400(mV), after that the current density increases abruptly till the end of the run, which may be due to localized corrosion .

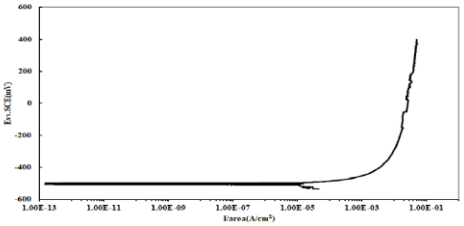

Figure (4) Potentiodynamic polarization curves of specimen (316L SS and CS) for as weld condition

Anodic polarization curves for aging specimens (316L SS and CS) in neutral pH solution are shown in figures (5-7). Anodic polarization curves shows that the current density increases with increasing the

applied potential till reaches almost constant value. This can interpreted to the changes on the surface of the alloy.

Figure (5) shows the anodic polarization curve for specimen (316L SS and CS) aging for 50 hr at 550 °C the corrosion current density I_{corr} is 5.2 E-3 (A/ $cm^{2)}$, the current density increases moderately till -500 mv, after that the current density increases till the end of the run. The corrosion current is higher than that of as weld condition.

Figure (6) shows the anodic polarization curve for specimen (316L SS and CS) aging for 500 hr at 550 °C , the corrosion current density I_{corr} is 6.44 E-6 (A/ $cm^{2)}$, the current density increases moderately till -400 (mV) in this case the current density increases steadily with content rate to the end of the experiment.

Figure (7) shows the anodic polarization curve for specimen (316L SS and CS) aging for 1000 hr. at 550 °C, the corrosion current density I_{corr} is 560.2 E-5(A/ cm^{2}), the current density increases moderately till certain potential, after this case the current density abruptly increases after corrosion potential with high rate.

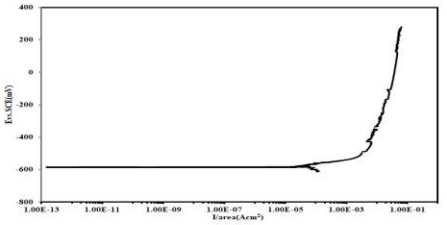

Figure (5) Anodic polarization curve in 3%NaCl solution of sample (316L SS and CS) aging for 50 hr at 550°C

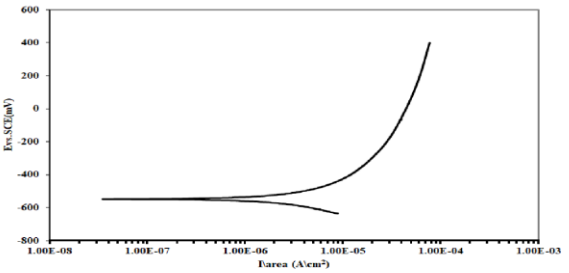

Figure (6) Anodic polarization curve in 3%NaCl solution of sample (316L SS and CS) aging for 500 hr at 550°C

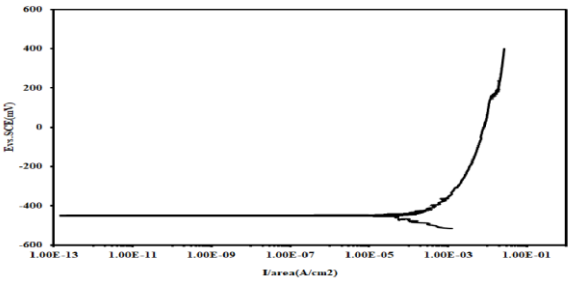

Figure (7) Anodic polarization curve in 3%NaCl solution of sample (316L SS and CS) aging for 1000 hr at 550°C

The major corrosion type that has been observed for all samples was localized corrosion. The corrosion current density (I_{corr}) of the different conditions of the samples varied in a very wide range from is 5.2 E-3(A/ $cm^{2)}$ to 6.44 E-6 (A/ cm^2) and the highest corrosion current density (I_{corr}) is for as weld condition. There were differences in the corrosion potential (E_{corr}) values for the samples aged for 1000 hr at 550 ˚C than the as weld condition.

Sung-Yu Kim et al [10] found that the low corrosion resistance of type 316L SS with δ-ferrite in the acidic solution is due to the lower concentrations of Cr and Mo in γ phase to cause galvanic corrosion in the active potential zone and to degrade the stability of passive film in the passive potential zone. In addition, the pitting resistance of type (316L SS) in the neutral pH solution is affected by inclusions such as sulfur compounds rather than δ-ferrite. [25]

The lower corrosion resistance of type (316L SS) with δ-ferrite phase is due to the lower concentrations of Cr and Mo in γ phase.

5- CONCLUSIONS

1. From Schaeffler diagram the weld microstructure for use (316L SS) fillers metal can be expected. Close to the fusion boundary, the SS clad region consisted of a narrow zone of fine dendrites of ferrite and austenite.
2. In this work, aging at temperature 550°C for different times varying from 50 hr to1000 hr, modifies the microstructure and corrosion behavior of austenitic stainless steel 316L. The microstructure changes occur in ferrite content.

3. Anodic polarization curves for specimens (316L SS and CS) for as weld condition and aging times 50,500 and 1000 hr at 550 °C in 3% NaCl solution with neutral pH were studied. The major corrosion type that has been observed for all samples was localized corrosion.
4. The corrosion current density (I_{corr}) of the different conditions of the (316LSS) varied in a very wide range from is 5.2 E-3(A/ cm^2) to 6.44 E-6(A/ $cm^{2)}$ and the highest corrosion current density (I_{corr}) is for as weld condition.

REFERENCES

1-Oliveira LA, Correa EO, Valeriano LC, et al. "Effect of weld metal chemistry on stress corrosion cracking susceptibility of austenitic AISI 316/ 2304 duplex stainless steels dissimilar weldment. Material Sci & Eng. (2018);2(6):281–285.
2-Iordachescu, Mihaela, Jesús Ruiz Hervías, Danut Iordachescu, Andrés Valiente Cancho, and Luis Caballero Molano. "Thermal influence of welding process on strength overmatching of thin dissimilar sheets joints." (2010).
3-Padilha, Angelo Fernando, Caio Fazzioli Tavares, and Marcelo Aquino Martorano. "Delta ferrite formation in austenitic stainless steel castings." In *Materials Science Forum*, vol. 730, pp. 733-738. Trans Tech Publications, 2013.
4-Rhouma, A. Ben, Tidiane Amadou, Habib Sidhom, and Chedly Braham. "Correlation between microstructure and intergranular corrosion behavior of low delta-ferrite content AISI 316L aged in the range 550–700° C." *Journal of Alloys and Compounds* 708 (2017): 871-886.
5-AF, Padilha. "Decomposition of austenite in austenitic stainless steels." *ISIJ international* 42, no. 4 (2002): 325-327.
6-Xiong, Qi, Hongjuan Li, Zhanpeng Lu, Junjie Chen, Qian Xiao, Jiarong Ma, and Xiangkun Ru. "Characterization of microstructure of A508III/309L/308L weld and oxide films formed in deaerated high-temperature water." *Journal of Nuclear Materials* 498 (2018): 227-240.
7-Saluja, Rati, and K. M. Moeed. "The emphasis of phase transformations and alloying constituents on hot cracking susceptibility of type 304L and 316L stainless steel

welds." *International Journal of Engineering Science and Technology*4, no. 5 (2012): 2206-2216.
8-Korinko, P. S., and S. H. Malene. "Considerations for the weldability of types 304L and 316L stainless steel." *Practical failure analysis* 1, no. 4 (2001): 61-68.
9-Shankar, V., T. P. S. Gill, S. L. Mannan, and S. Sundaresan. "Solidification cracking in austenitic stainless steel welds." *Sadhana* 28, no. 3-4 (2003): 359-382
10- Sung-Yu Kim, Hyuk-Sang Kwon and Heesan Kim,"Effect of delta ferrite on Corrosion Resistance of Type 316L Stainless Steel in Acidic Chloride Solution by Micro-droplet Cell" Solid State Phenomena Vols. 124-126 (2007) pp 1533-1536
11-Dadfar, M., M. H. Fathi, F. Karimzadeh, M. R. Dadfar, and A. Saatchi. "Effect of TIG welding on corrosion behavior of 316L stainless steel." Materials Letters 61, no. 11-12 (2007): 2343-2346.
12-Schaeffler, A. L" Constitution diagram for stainless steel weld metal". Meta Progress(1949). 56(11): 680–680B.
13-Long, C. J., and DeLong, W. T."The ferrite content of austenitic stainless steel weld metal". *Welding Journal (*1973)52(7): 281-s to 297-s.
14-Siewert, T. A., McCowan, C. N., and Olson, D. L."Ferrite Number prediction to 100 FN in stainless steel weld metal". *Welding Journal(*1988) 67(12): 289-s to 298-s.
15-Kožuh, Stjepan, M. Gojic, and Ladislav Kosec. "Mechanical properties and microstructure of austenitic stainless steel after welding and post-weld heat treatment." *Kovove Materialy* 47, no. 4 (2009): 253-262.
16- David S. A., Goodwin G.M. "Solidification behaviour of austenitic stainless steel filler metals." Weld Journal. (1979): 58: 330s–336s.
17-Song, Y., and McPherson NA. "The effect of welding process on the chi phase precipitation in As-Welded 317L Weld Metals." *ISIJ international* 36, no. 11 (1996): 1392-1396.
18-Bermejo, M. Asunciòn Valiente. "Predictive and measurement methods for delta ferrite determination in stainless steels." *Welding journal* 91 (2012): 113.
19-Şimşir, Mehmet, Levent Cenk Kumruoğlu, and Ali Özer. "An investigation into stainless-steel/structural-alloy-steel bimetal produced by shell mould casting." *Materials & Design* 30, no. 2 (2009): 264-270.

20-Kim, Sung Yu, Hyuk Sang Kwon, and Hee San Kim. "Effect of delta ferrite on corrosion resistance of type 316L stainless steel in acidic chloride solution by micro-droplet cell." In *Solid State Phenomena*, vol. 124, pp. 1533-1536. Trans Tech Publications, 2007.

21-Hajian, M., A. Abdollah-Zadeh, S. S. Rezaei-Nejad, H. Assadi, S. M. M. Hadavi, K. Chung, and M. Shokouhimehr. "Microstructure and mechanical properties of friction stir processed AISI 316L stainless steel." *Materials & Design* 67 (2015): 82-94.

22-Bai, Guanshun, Shanping Lu, Dianzhong Li, and Yiyi Li. "Intergranular corrosion behavior associated with delta-ferrite transformation of Ti-modified Super304H austenitic stainless steel." *Corrosion Science* 90 (2015): 347-358.

23-Saluja, Rati, and K. M. Moeed. "Formation, quantification and significance of delta ferrite for 300 series stainless steel weldments." *International Journal of Engineering Technology, Manage-ment and Applied Sciences* 3 (2015): 23-36.

24-Korinko, P. S., and S. H. Malene. "Considerations for the weldability of types 304L and 316L stainless steel." *Practical failure analysis* 1, no. 4 (2001): 61-68.

25-Rustandi, Andi, and Suganta Setiawan. "The Effect of Ferrite Content on Mechanical Properties and Corrosion Behaviour of Austenitic Stainless Steel 308L Weld Metal." In *Solid State Phenomena*, vol. 263, pp. 108-114. Trans Tech Publications, 2017.